IFASD 2015
International Forum
on Aeroelasticity and Structural Dynamics
June 28 — July 02, 2015 ▲ Saint Petersburg, Russia

MULTIPLE INPUT DSCRIBING FUNCTION ANALYSIS OF NON-CLASSICAL AILERON BUZZ

M. Irfan Zafar, Francesca Fusi[2], Giuseppe Quaranta[3]

Dipartimento di Scienze e Tecnologie Aerospaziali
Politecnico di Milano
Campus Bovisa Sud
via La Masa, 34
20165 - Milano
[2] francesca.fusi@polimi.it
[3] giuseppe.quaranta@polimi.it

Keywords: computational aeroelasticity, describing function, aileron buzz, fluid structure interaction, limit cycle oscillation

Abstract: This paper focuses on the computational study of nonlinear effects of unsteady aerodynamics for non-classical aileron buzz. It aims at a comprehensive investigation of aileron buzz phenomenon under varying flow parameters utilizing the classical approach of describing function technique with multiple input variables. Limit cycle oscillatory behavior of an asymmetrical airfoil section has been studied initially using an expensive high-fidelity model basd on a coupled CFD/CSD time marching approach. Using this high fidelity model, a multiple input aerodynamic describing function was developed that can effectively represent lumped nonlinearities of aerodynamic subsystem. Limit cycles can be closely identified through multiple input aerodynamic describing function representation, taking into account also the bias effect due to the use of non-symmetric airfoils. Traditional LCO analysis of sensitivity with respect to hinge moment of inertia is performed. Further, outburst points of limit cycle amplitude for varying Mach number and angle of attacks are investigated. By using developed aerodynamic describing function, it has been demonstrated that limit cycle analysis methods may still be used while including the effects of aerodynamic nonlinearities. Results from both methods, direct time marching and multiple input describing function, have been broadly compared for validation.

1 INTRODUCTION

Transonic flight regime inherently involves nonlinear flow phenomena due to the simultaneous presence of locally subsonic and supersonic regions, shock waves and flow separation which presents various challenging aeroelastic problems that need to be tackled for the design of more efficient and safer aircrafts. Interaction of flow with a moving structure leads to spatial variation of shock waves and flow separation points, hence consequently to unsteady flow behavior. For small perturbations about steady flow, flow variables and shock waves' positions vary in a linear

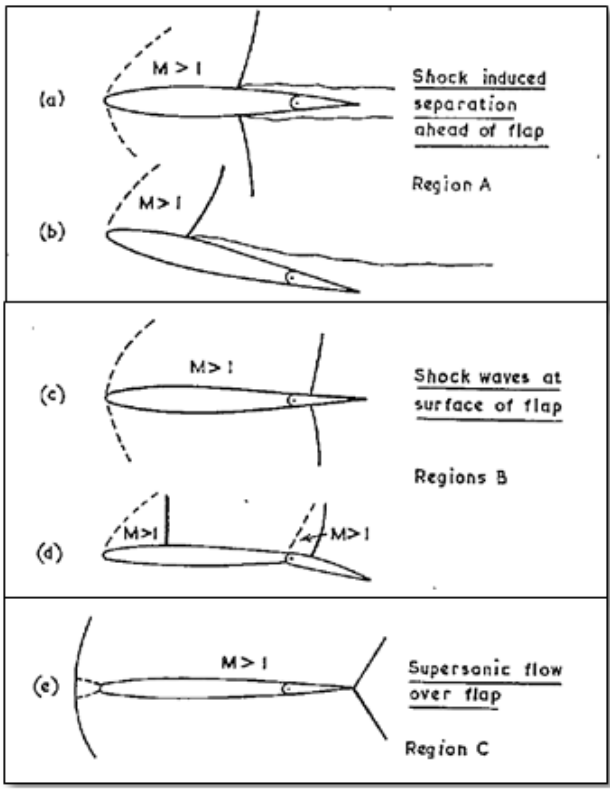

Figure 1: Buzz related Flow Regimes, from Ref. [3].

fashion with the wing/control surface motion. But when the wing/control surface motion is large enough to cause large variation of shock wave position or separation of boundary layer, linear assumption is not correct anymore. Consequently unsteady aerodynamic forces exhibit nonlinear behavior.

Non-linear interaction of control surface motion with the variation in shock waves' position and flow separation is referred to as *buzz*. Aileron buzz is a one degree of freedom flutter involving self-excited oscillations of aileron about its hinge, caused by the unsteady aerodynamics related to shock wave dynamics and shock boundary layer effects. Aileron buzz, being an exception among few single degree-of-freedom instabilities, may results in explosive flutter with very large amplitudes within a few cycles and which in some tests have led to permanent damage to the aileron and/or wing involved in the test [1, 2].

Aileron Buzz can be classified as done by Lambourne [3] for viscous flows, as Type A, B and C, on the basis of whether the shock waves are ahead of the hinge, on the aileron surface or at the trailing edge and the corresponding mechanisms of buzz excitation, as is sketched in Figure 1. With respect to Type B, Lambourne explained that boundary layer separation was observed, but it did not appear to be the driving mechanism. A later work by Bendiksen [4] endorsed the idea that in such condition buzz is driven by dynamics of shock waves moving over aileron surface. This type of buzz is called *non-classical aileron buzz* to emphasize the observance of the instability even in the case when boundary layer separation and shock-boundary layer interaction are not modeled.

Development of accurate and efficient models to investigate nonlinear phenomena like aileron buzz involving unsteady aerodynamics has been a focus of research for years. Experimental techniques have a major disadvantage that should the susceptibility of such dynamic instability being identified, redesign must take place in the late development phase which tends to be extremely expensive. Numerical simulations using high-fidelity CFD codes coupled with appropriate structural model have proven to be accurate enough to analyze/compute nonlinearities involved in the unsteady aerodynamics of aileron buzz [4, 5]. However standard Computational Fluid Dynamics(CFD) models that include the relevant fluid nonlinearities are simply too expensive now and for some time to come for most aeroelastic analyses. Thus there has been much interest in reducing computational costs while retaining the essence of the nonlinear flow phenomenon.

Several ideas have been pursued in retaining the accuracy associated with state-of-the-art CFD models while reducing model order and computational cost. Dynamically linear approximations are considered when the shock motion or the flow separation point motion is linearly proportional to the motion of the structure. This is sufficient to assess the linear stability of the aeroelastic system but not to determine LCO amplitudes due to nonlinear aerodynamic effects [6]. To analyze the nonlinear aerodynamic effects, the idea of transfer functions is exploited to create small computational models from large CFD codes. Under this class falls the classical Describing Function (DF) technique, which requires the quasi-linearization, of lumped nonlinearity in the aeroelastic system.

In this perspective, current study is focused on a comprehensive investigation of shock wave dynamics' role in the non-classical aileron buzz using high-fidelity CFD code which is exploited also to develop an aerodynamic describing function which effectively predicts the LCO characteristics while retaining the accuracy associated with expensive CFD models. This research effort will be presented as follows: Section 2 will present an overview of the high-fidelity numerical model based on CFD while section 3 will analyze the results formulated using this numerical model. Section 4 will detail the evaluation of aerodynamic describing function and a comparative analysis of the results when CFD model is replaced by DF representation.

2 NUMERICAL MODEL

To accurately solve this non-linear aeroelastic problem, it is necessary to use sophisticated mathematical model and numerical methods within the very active research field of Computational Aeroelasticity (CA). The aeroelastic computational model used in the current study is the result of the coupling between the structural dynamics of the aileron which provides the displacements, namely the aileron deflection angle β and the aerodynamic model which gives the aerodynamic load acting on the control surface namely the hinge moment M_H. Aeroelastic system of aileron buzz is modeled as shown in Figure 2. The dynamic model is represented by a fixed wing section of asymmetrical airfoil. Aileron is integrated into the wing. It is hinged at three-quarter-chord location and its rotation about hinge is modeled as rigid. Positive sense of aileron deflection and hinge moment are oriented downwards as shown in Figure 2(a).

2.1 Aerodynamic Model

In order to accurately study nonlinear aerodynamics effects, high-fidelity CFD solver uses the mathematical model of the Euler Equations as it is capable of representing the shock waves'

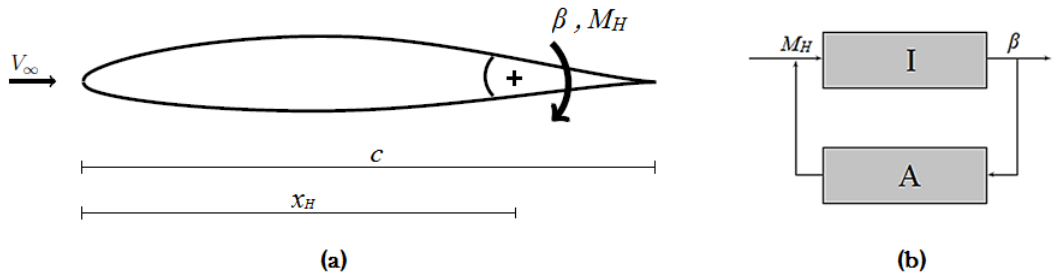

Figure 2: Dynamic System

dynamics which drive the instability in the case of non-classical aileron buzz. Furthermore, the simulation of aileron buzz requires to compute unsteady flow field in which the computational domain is continuously changing its shape to account for the control-surface motion. Therefore, it is necessary to resort to the Arbitrary Lagrangian Eulerian (ALE) formulation of the Euler equations

$$\frac{d}{dt}\int_{\Omega(t)} \mathbf{u} d\Omega + \oint_{\Gamma(t)} [\mathbf{f}(\mathbf{u}) - \mathbf{u}\nu] \cdot \mathbf{n} d\Gamma = 0 \tag{1}$$

that is completed by suitable initial and boundary conditions. $\Omega(t) \subseteq \mathbb{R}^2$ is the moving spatial domain and $\Gamma(t) = \partial\Omega(t) \subseteq \mathbb{R}$ represents the boundary having normal unit vector $\mathbf{n}(\mathbf{x}, t)$ pointed outwards. Vector $\mathbf{u}(\mathbf{x}, t)$ stores the unknown conservative variables, i.e. density, momentum and total energy, while vector $\mathbf{f}(\mathbf{u})$ includes the inviscid flux functions and vector $\nu(t)$ represents the local velocity of all the moving boundaries [7]. The finite volume discretization in space of Eq.1 yields a set of ordinary differential equations in time, whose solution provides the pressure field around the wing section and thereby the time-varying aerodynamic moment acting on the aileron. For numerical implementation, `AeroFoam` solver is used, whose development started back in 2008 and continues today [8]. The aerodynamic grid is a C-mesh built around the wing section and it is smoothly refined in radial sense from the far-field boundary to the body and around the hinge line.

2.2 Structural Model

Structural model is represented by rigid aileron integrated into the two dimensional wing section. Aileron motion is described by single degree of freedom motion about its hinge namely aileron deflection angle $\beta(t)$, with the governing equation for dynamics of structural model given as:

$$I_H \ddot{\beta}(t) = M_H(t) \tag{2}$$

where I_H is the aileron moment of inertia and $M_H(t)$ is the aerodynamic moment acting on the aileron, both evaluated with respect to the hinge line. Above equation provides the balance between inertial and aerodynamic forces, whereas structural elastic and dissipative contributions are not modeled in the present work. For an asymmetrical airfoil is under consideration, the initial condition for the equation is a perturbation provided by the initial steady unbalanced aerodynamic moment acting on the aileron while it is at zero-deflection angle.

Aeroelastic interface is based on the fact that the airfoil is rigid. Hence at each time instant,

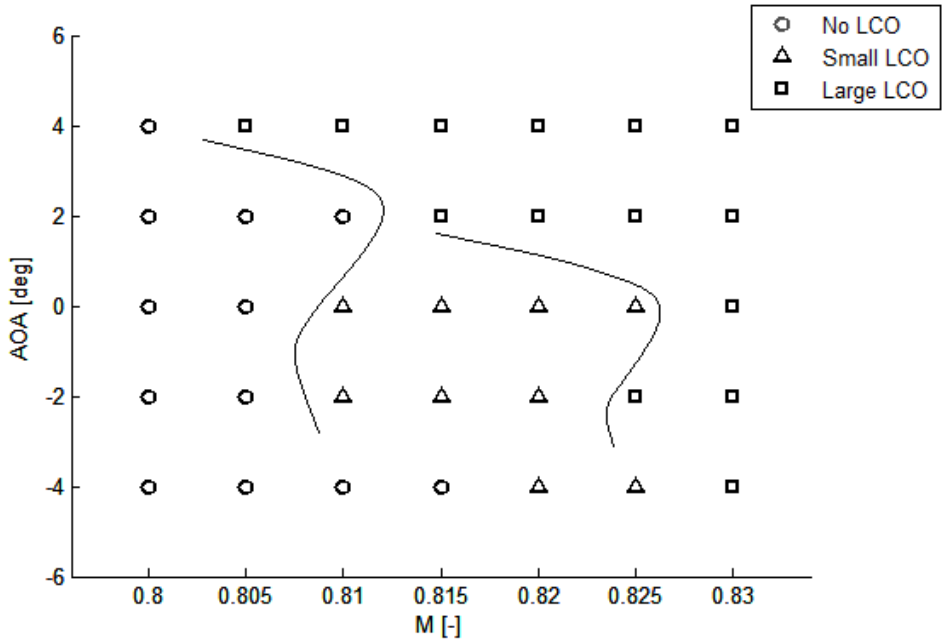

Figure 3: LCO points

aileron deflection angle is calculated and the displacements of the boundary cells surrounding aileron are related to the aileron deflection angle through a rotation operator. Defined structural displacement and velocity field are then translated into variation of the boundary conditions of the aerodynamic subsystem through aeroelastic interface operator.

For the present study, two dimensional wing section has been used for the current study as has been done extensively for such aeroelastic problems, both in numerical simulations and wind tunnel tests [2, 4]. Computations have been performed for an asymmetrical airfoil NACA 65-213. This choice of airfoil is based on the availability of the necessary data for buzz simulation along with some historical perspective available also for the same airfoil. Earliest indication of presence of control surface buzz phenomenon was established by flight tests of P-80 jet fighter aircraft whose airfoil shaping resembled with NACA 65-213. Required data for buzz simulation was obtained from Ref. [9], which specifies airfoil chord (c) = 1.472 m, aileron moment of inertia $(I_H) = 0.5536$ kg m^2 and Reynolds number $(Re) = 1.10^7$.

3 TEST AND RESULTS

The reliability of the presented numerical model and problem setup haxs been extensively established by earlier research works [8, 10] through various tests and by tackling set of realistic static and dynamic aeroelastic problems.

For the current problem setup, responses computed at incrementing Mach numbers and range of angles of attack show a pattern of buzz appearance after free play, once set free from initial condition of zero-deflection angle ($\beta = 0$). Figure 3 shows the set of Mach numbers and angles of attack that lead to limit cycle oscillations of small or large amplitudes under prescribed initial conditions. For the reason of asymmetric shape of wing section, appearance of small and correspondingly large limit cycle oscillations can be observed to be appearing at lower Mach

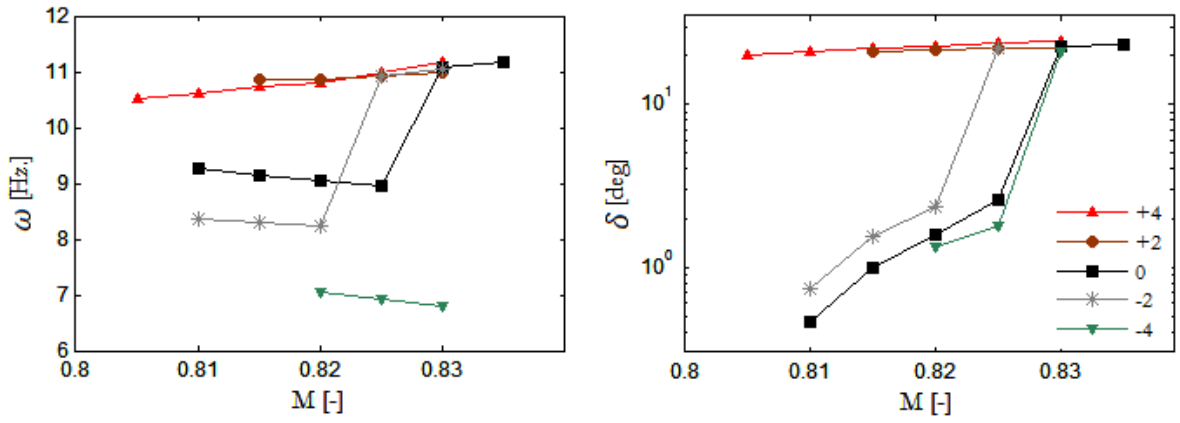

Figure 4: LCO frequency (ω) and amplitude (δ) (logarithmic scale) variation

numbers for positive angles of attack and at delayed Mach numbers for negative angles of attack. Further knowledge of LCO characteristics at these points especially the amplitude of oscillation is of critical importance. Figure 4 shows the variation of these characteristics where outburst in limit cycle amplitude can be observed along with corresponding increase in frequency. Further insight into this intriguing nature of interaction between shock wave dynamics and aileron free-play will aid in formulating the interplay between wing section's asymmetric shape, relative motion of shock waves and consequently LCO characteristics.

Figure 5 assists in understanding the spatial variation of shock waves with incrementing Mach number. For Mach numbers just above the critical one, stationary shocks' positions are effected solely by the camber of the airfoil, that is upper shock is relatively ahead of lower shock wave even after aileron has negative (upwards) deflection for mean position. As Mach number increases, and consequently shocks get closer to the aileron, lower shock settles ahead of upper shock being effected by the aileron's upwards deflection. As long as aileron can settle to mean deflection (for zero-hinge moment) with out locating shock wave/s on its surface, buzz isn't incited. Further increase in Mach number results in aileron interaction with moving shock waves wherein the shock motion interacts with the aileron to extract energy from the fluid that leads to buzz occurrence.

While the amplitude of oscillation increases with increasing Mach number, critical information is the condition when this amplitude escalates to very high values. Careful observations show that this case occurs when either increase in Mach number or geometrical effects causes the upper and lower shock waves, both, to partially move over aileron. From Figure 5, it is evident that until M=0.825, unlike lower shock wave, upper shock hasn't started moving over aileron and LCO amplitude is of lower order. However another increment in Mach number (i.e. M=0.83) causes upper shock also to move over aileron that leads to outburst in oscillation amplitude. Similar observations can be traced from Figure 6 where results computed at angle of attack negative 2 degrees emphasize the fact that explosive amplitude for buzz is absent until upper shock also starts interacting with aileron by partially moving over it along with lower shock.

Results of spatial variation of shock waves at positive 2 degrees angle of attack, shown in Figure 7, signifies the cases where large amplitude limit cycle oscillation can also be incited by geometrical effects. Simulation have shown expansion waves being generated at lower surface, incited from an edge appearing in the geometry at hinge location due to the aileron deflection.

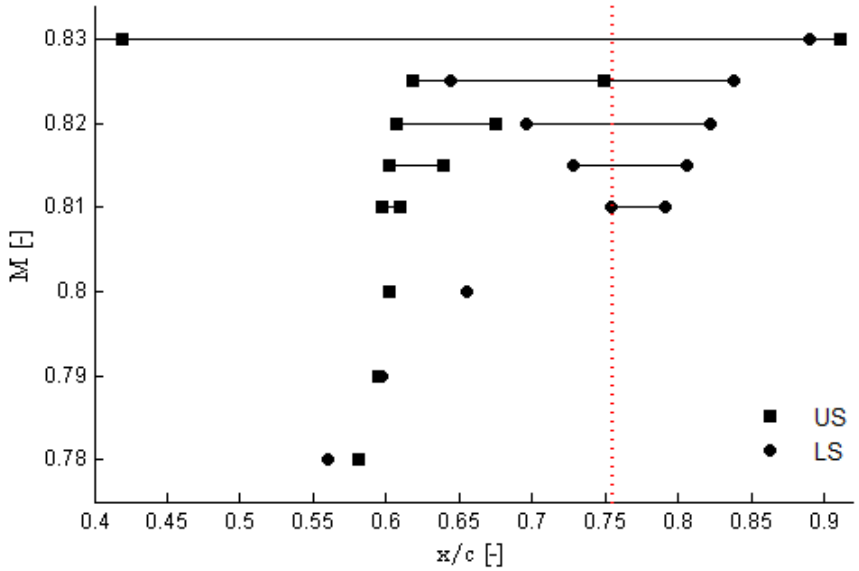

Figure 5: Spatial variation of upper shock (US) and lower shock (LS) for AOA=0 deg; Hinge location represented by red line

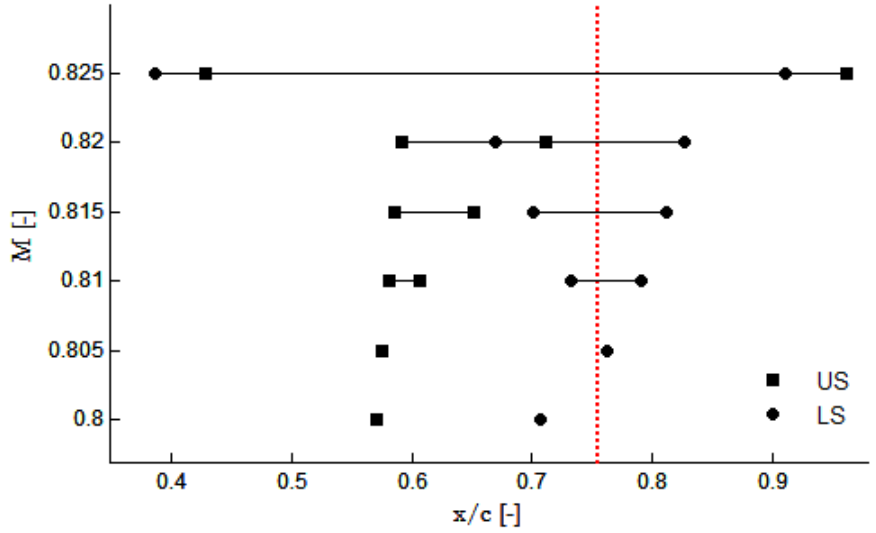

Figure 6: Spatial variation of upper shock (US) and lower shock (LS) for AOA=-2 deg. Hinge location represented by red line

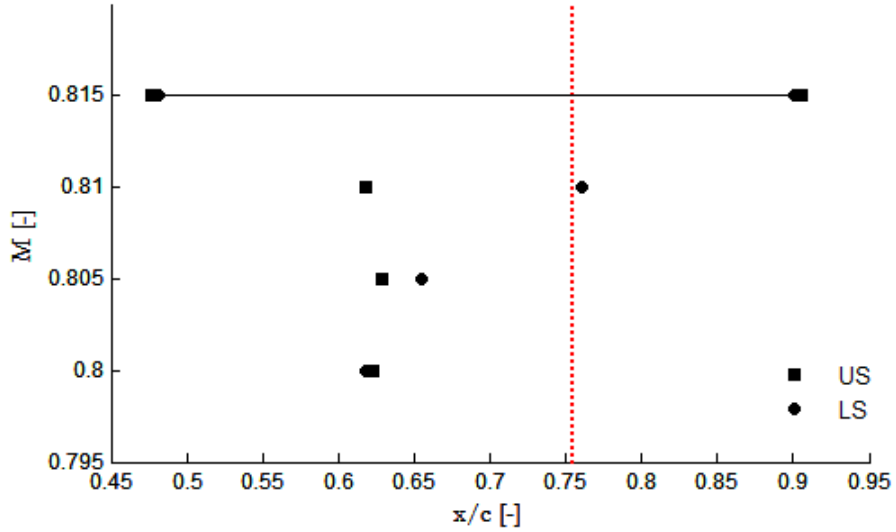

Figure 7: Spatial variation of upper shock (US) and lower shock (LS) for AOA=+2 deg. Hinge location represented by red line

At some angle of attack and Mach number combinations, these expansion waves may result in generation of shock wave directly on the aileron surface which again escalates the oscillation amplitude. So in the case of Mach number 0.815 in Figure 7, lower shock develops on the aileron, moves a bit on the aileron and then vanishes in one cycle of oscillation unlike upper shock which is moving back and forth of aileron hinge. So in this case, large LCO can be attributed to geometrical effects and initial perturbation which deflected aileron enough to create an edge.

The amplitude outburst can be put into perspective by studying the moment being imparted to the aileron by pressure distribution and the time lag associated with the aerodynamics response to structural displacement. Incidentally this pressure distribution interacts with aileron motion in such a way that energy is imparted from fluid to structure, owing to the time lag, hence leading to higher negative aerodynamic damping (hence net negative damping).

To emphasize this point, momentary C_P distributions have been compared with aileron deflection in Figure 8, where two instants in time are chosen. When a shock wave is located on the aileron, part of aileron is effected by supersonic region (very low pressure coefficient) hence imparting significant net moment to aileron. At time instant 0.11, aileron is moving upwards, meanwhile presence of upper surface shock at aileron impart energy such that it acts as a push for aileron to achieve greater amplitude in the direction of motion. Similar scenario can be observed for time instant 0.15 when aileron motion is augmented by shock waves' position. This augmentation leads to sudden increase in amplitude and potentially fatal oscillations in very few cycles.

Results discussed above show the nonlinear behavior with respect to the shock waves' positional interplay. Characteristics of buzz have been found to be highly dependent on initial perturbation of flow hence displacement of aileron from mean position. In addition to that geometrical aspects like asymmetrical shape of wing section and edge appearance on airfoil surface have significant effects. These results show the vulnerability of transonic regime to various flow

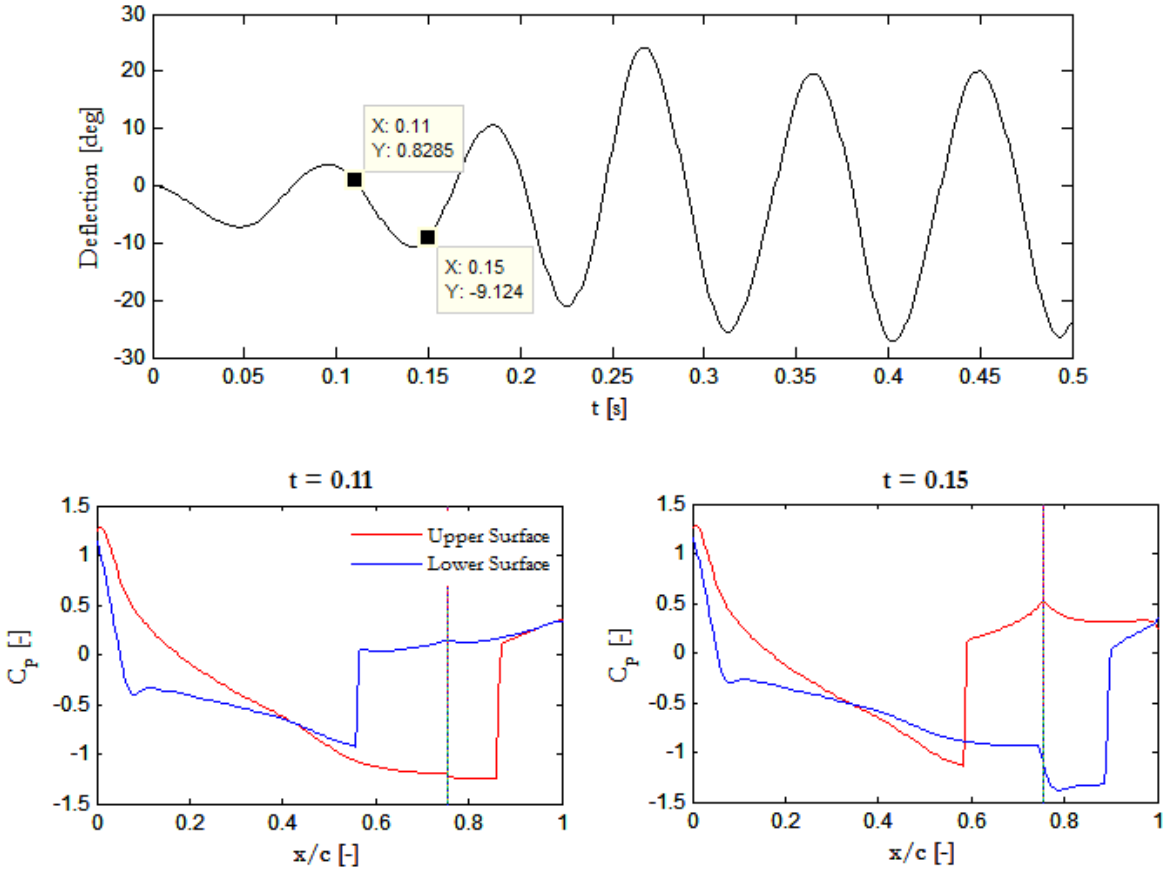

Figure 8: Momentary relation between aileron motion and shock location

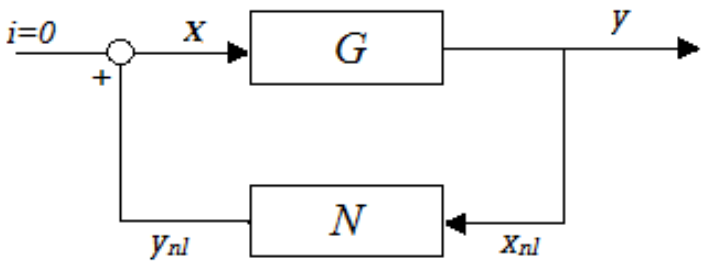

Figure 9: Quasi-linearized system

phenomena which can be incited under flow conditions as well as geometrical circumstances.

4 AERODYNAMIC DESCRIBING FUNCTION

Describing Function (DF) technique provides the ease of approximating nonlinear system under investigation by a quasi-linear model. In this approach, the form of Describing Function (DF) is assumed and the coefficients are determined from the data generated by the CFD code in time simulation. This type of quasi-linear system retains the possibility of sharing some analysis methods typical of linear systems.[11]

For Describing function to be apt to reproduce the overall nonlinear response, the linear part of the system should act as a low pass filter with passband low enough to rule out higher harmonics out of the response. This low-pass filtering hypothesis is usually verified but it is rarely possible to check it up front, and so the DF method is often considered an empiric approach.

Approximation of aerodynamic subsystem's nonlinearity by a describing function can be demonstrated well through Figure 9, which shows aeroelastic system of aileron buzz where linear element (structural subsystem) is characterized by its frequency response function $G(j\omega)$ and the nonlinear element (aerodynamic subsystem) by its Describing Function $N(\omega, \delta, \gamma)$ representation.

Structural subsystem $G(j\omega)$ takes aerodynamic moment as input and aileron deflection angle as the output. Frequency response function (FRF) for this linear element can be obtained as:

$$G(j\omega) = \frac{\beta(j\omega)}{M_H(j\omega)} = -\frac{1}{I_H\omega^2} \tag{3}$$

Comparing aeroelastic system in Figure 9 with a typical feedback system, system's output must closely approximate nonlinearity input to have a good representation through describing function. For oscillatory behavior of an asymmetrical airfoil, sinusoidal signal plus a bias can be considered as an appropriate form of the nonlinearity input:

$$x_{nl}(t) = \gamma + \delta sin(\omega t) \tag{4}$$

which has a bias component γ and a periodic component with frequency ω and amplitude δ. The functions $\gamma,\ \delta$ and ω are determined by the nature of the system and its inputs. The output

can be expressed by using a Fourier series:

$$y_{nl}(t) = \sum_{n=0}^{\infty} |A_n(\omega, \delta, \gamma)| \; sin[n\omega t + \phi(\omega, \delta, \gamma)]$$

where A_n are Fourier coefficients. Such coefficients are functions of input frequency, bias and amplitude because they describe the output of a nonlinear element. Nonlinearity output can be further distributed into the following form:

$$y_{nl}(t) = y_a(t) + y_r(t)$$

where $y_a(t)$ takes care of the contributions of a constant and fundamental frequency terms ($n = 0, 1$) and $y_r(t)$ denotes the contributions of higher harmonics ($n > 1$). The output after passing through the linear element, takes the form as:

$$y(t) = G.y_a(t) + G.y_r(t)$$

Prescribed and free oscillation responses validate the hypothesis of filtering characteristics of loop linear part, that it significantly attenuates higher harmonics. Under this important approximation, higher harmonics contribution can be neglected as:

$$G.y_a(t) \gg G.y_r(t)$$

So, nonlinearity output can be represented by considering only the first harmonic term plus bias and following form of Dual Input Describing Function can be obtained:

$$y_a(t) = N_\gamma \gamma + [\Re[N_\delta] sin(\omega t) + \Im[N_\delta] cos(\omega t)]\delta \tag{5}$$

where N_γ and N_δ are approximating gains to bias and sinusoidal input components respectively and are given as:

$$N_\gamma(\omega, \delta, \gamma) = \frac{A_0(\omega, \delta, \gamma)}{\gamma}$$

and

$$N_\delta(\omega, \delta, \gamma) = \frac{|A_1(\omega, \delta, \gamma)|}{\delta} e^{j\phi(\omega,\delta,\gamma)}$$

N_δ is generally defined as the complex fundamental-harmonic gain of a nonlinearity in the presence of a driving sinusoid. These gains/coefficients will be evaluated from the system's response to prescribed input variables for set of values. DF gains are then related to varying input variables using Cubic Spline interpolation.

From the presented representation of the structural and aerodynamic subsystems, quasi-linearized aeroelastic system output can be formulated as:

$$y(t) = G y_{nl}(t) \cong G y_d(t)$$

$$\begin{aligned} y(t) \;\cong\; G(j0) N_\gamma.\gamma \;\; & + (\Re[G(j\omega)] \{\Re[N_\delta] sin(\omega t) + \Im[N_\delta] cos(\omega t)\} \\ & + \Im[G(j\omega)] \{\Re[N_\delta] sin(\omega t) + \Im[N_\delta] cos(\omega t)\})\delta \end{aligned}$$

At the limit cycle condition, $y(t) = x_{nl}(t)$, which leads to following set of equations:

$$G(j0) \; N_\gamma(\omega, \delta, \gamma).\gamma = \gamma \tag{6}$$

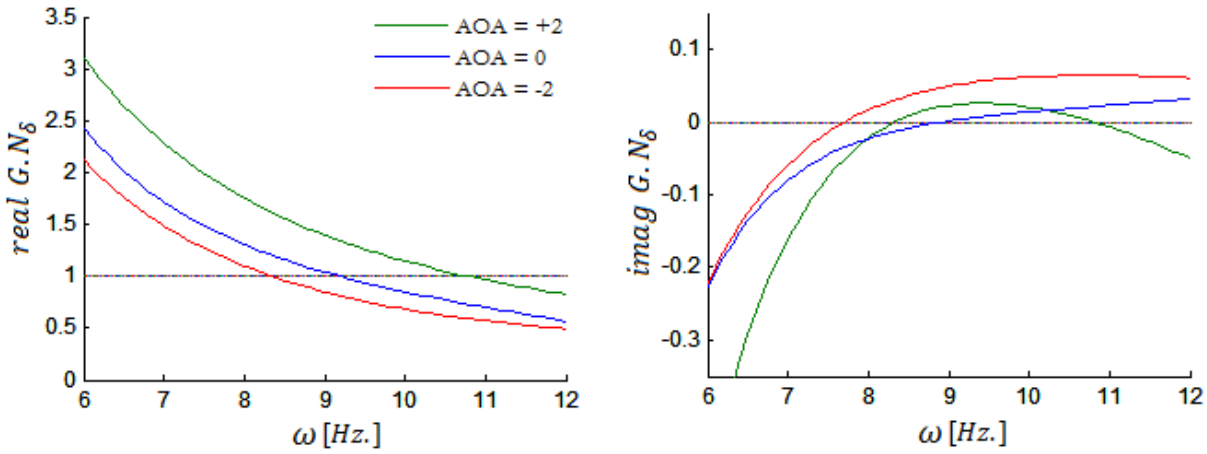

Figure 10: Variation of real and imaginary components of complex harmonic gain (N_δ) w.r.t frequency(ω)

$$G(j\omega)\ \{\Re[N_\delta]\ sin(\omega t) + \Im[N_\delta]\ cos(\omega t)\ \}.\delta = \delta\ sin(\omega t) \tag{7}$$

Above two equations states the conditions for bias and sinusoidal contributions, respectively, to propagate identically around the loop for limit cycle to be established. For non-zero mean($\gamma \neq 0$) of unsymmetrical airfoil and static gain $G(j0) \rightarrow \infty$:

$$N_\gamma(\omega, \delta, \gamma) = 0 \tag{8}$$

which gives the condition for bias value which must be fulfilled to sustain limit cycle. Condition defined with respect to the sinusoidal component in Eq. 7, can be further segregated such that Eq. 7 gives:

$$G(j\omega).\Re[N_\delta(\omega, \delta, \gamma)] = 1 \tag{9}$$

$$G(j\omega).\Im[N_\delta(\omega, \delta, \gamma)] = 0 \tag{10}$$

Above three equations, i.e. Eq. 8, 9 & 10, form the set of three real nonlinear algebraic equations that is needed to be solved in order to compute three unknown parameters characterizing the limit cycle oscillations, which are bias, amplitude & frequency [12].

Aerodynamic describing function has been evaluated at number of Mach numbers and angles of attack conditions. Behavior of the real component concerning Eqn. 9 and the imaginary component concerning Eqn. 10 of complex fundamental harmonic gain (N_δ) with respect to frequency (ω) has been shown separately in Figure 10 and 11 where convergence can be achieved when both components equate to 1 and 0 respectively along with the satisfaction of Eqn. 8.

Variation of this complex fundamental harmonic gain with respect to amplitude (δ) in Figure 12 shows a rather comprehensive view of how these equations lead to predicting small and large amplitudes of oscillation.

Using this evaluated aerodynamics describing function, DF linearized aeroelastic system was formulated to predict LCO parameters and their variation with reasonable accuracy compared to the ones computed through CFD-based aeroelastic computations. Figure 13 and 14 show the

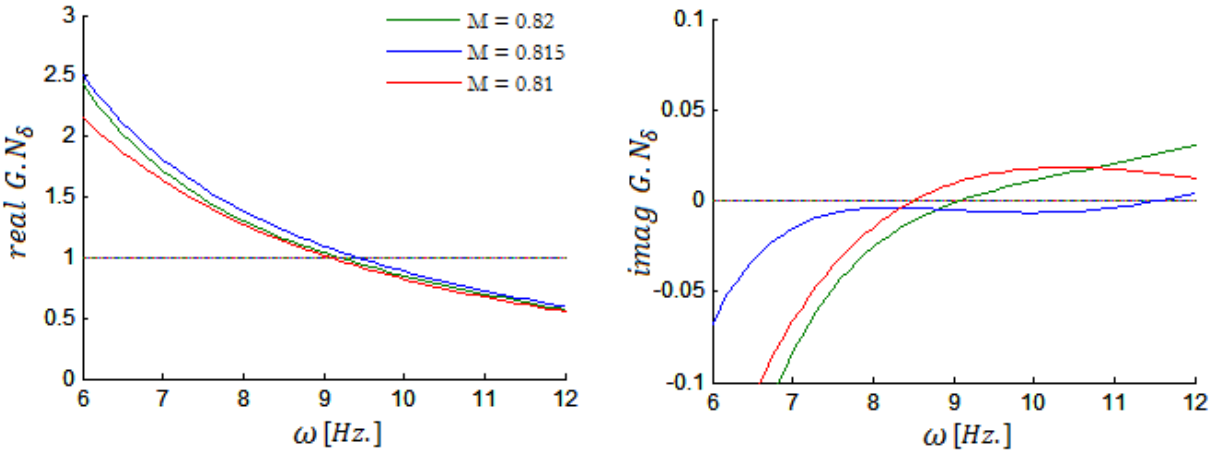

Figure 11: Variation of real and imaginary components of complex harmonic gain (N_δ) w.r.t frequency(ω)

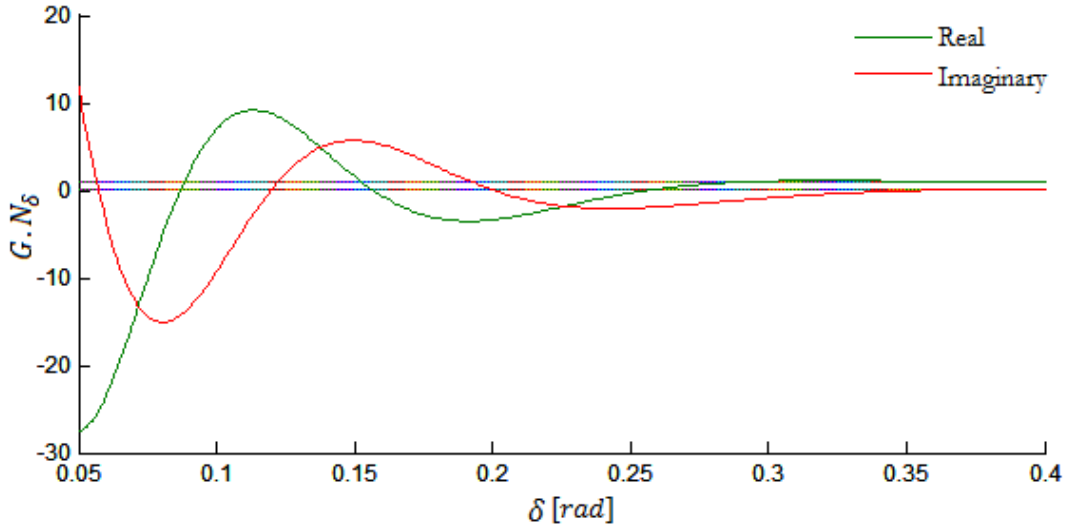

Figure 12: Variation of real and imaginary components of complex harmonic gain (N_δ) w.r.t amplitude(δ) at Mach number 0.82 and Angle of Attack of 2 deg

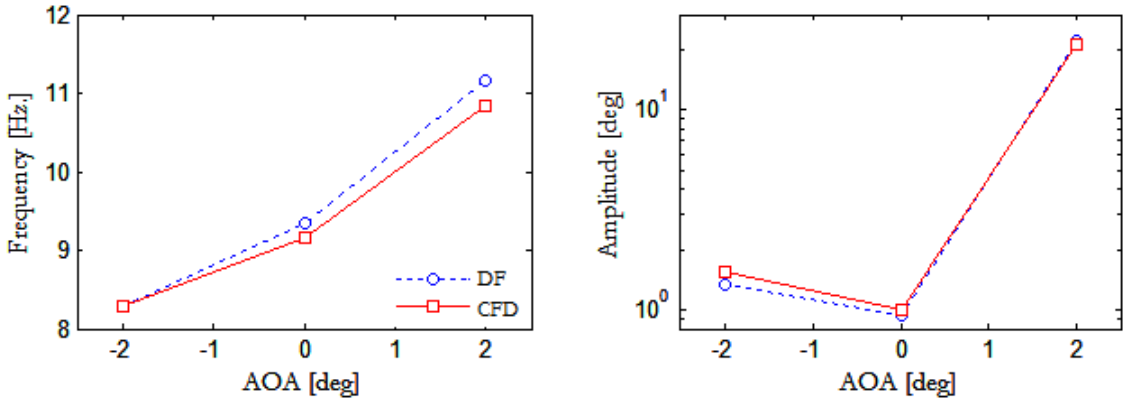

Figure 13: Aeroelastic system response comparison at Mach No. 0.815

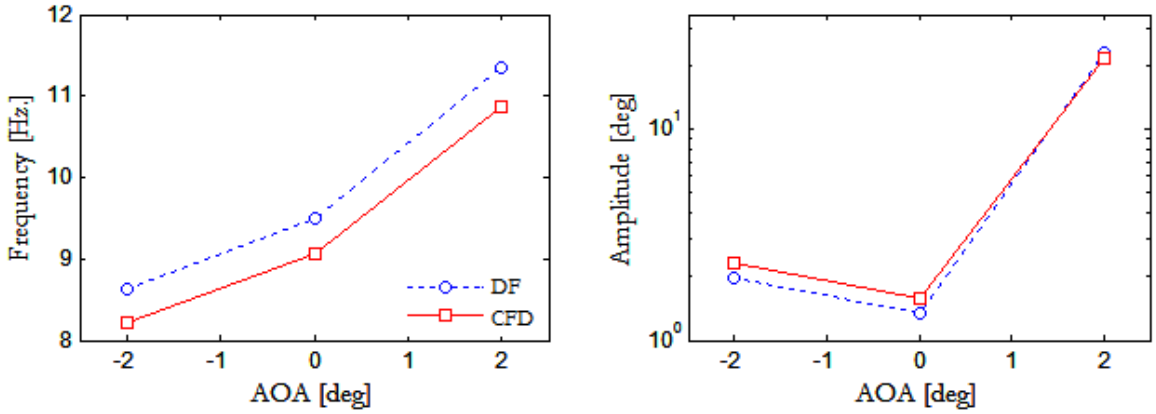

Figure 14: Aeroelastic system response comparison at Mach No. 0.82

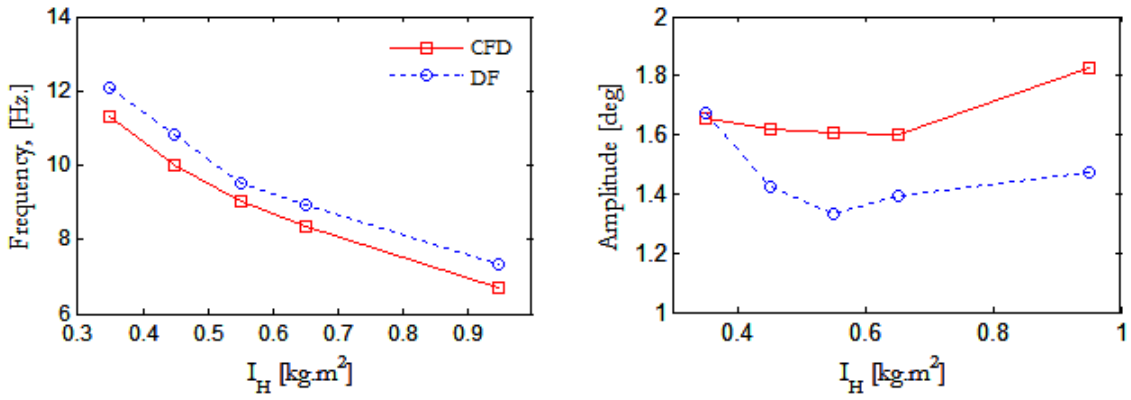

Figure 15: LCO characteristics variation with Hinge Moment of Inertia (I_H)

comparisons of the evaluated values at set of angles of attack. DF linearized aeroelastic system predicts the variation of the LCO characteristics with good accuracy and with little discrepancies in exact values. These results show the potential of describing function technique to develop reduced order representation of aerodynamic nonlinearity in the case limit cycle oscillation.

Developed linearized aeroelastic system should also be able to predict variation in limit cycle characteristics with respect to design variables, that in our case is hinge moment of inertia. This verification has been performed and the results have been shown in Figure 15 where significant variation in limit cycle frequency is observed with respect to hinge moment of inertia and this variation has been predicted with good accuracy. Limit cycle amplitude has been under-predicted however its dependence on hinge moment of inertia is observed to be rather low relative to the frequency. These results presents describing function technique as a powerful approach for non-linear aerodynamic modeling and predicting the characteristics of limit cycle oscillation.

5 CONCLUSIONS

This work investigates the nonlinear interaction between aileron free-play and shock wave dynamics which is the driving mechanism for non-classical aileron buzz. Results give a detailed insight of the interplay between asymmetrical shape of wing section, spatial motion of shock waves with respect to various flow conditions and excitation of aileron buzz. Characteristics of incited oscillations have been found to be highly dependent on initial perturbation and geometrical aspects of the wing section (asymmetry and edge appearance). Further, classical technique of Describing Function has been exploited to evaluate quasi-linearized representation of aerodynamics nonlinearities involved in the case of non-classical aileron buzz. Formulated DF linearized aeroelastic system predicts limit cycle oscillation characteristics with appreciable accuracy.

6 REFERENCES

[1] Saito, H. (1959). On the aileron buzz in transonic flow. Tech. Rep. 25 (6), Aeronautical Research Institute, University of Tokyo.

[2] Lambourne, N. C. (1958). Some instabilities arising from the interactions between shock waves and boundary layers. Tech. Rep. 182, AGARD.

[3] Lambourne, N. C. (1962). Control-surface buzz. Tech. Rep. 3364, Her Majesty Stationery Office.

[4] Bendiksen, O. O. (1993). Nonclassical aileron buzz in transonic flow. In *34th AIAA(ASME/ASCE/AHS/ASC Structures, Structural Dynamics and Materials Conference, AIAA/ASME Adaptive Structures Forum*, AIAA 93-1479. La Jolla, CA.

[5] Steger, J. L. and Bailey, H. E. (1980). Calculation of transonic aileron buzz. *AIAA Jorurnal*, 18(3), 249–255.

[6] Fusi, F., Romanelli, G., Guardone, A., et al. (2013). Nonlinear reduced order models of unsteady aerodynamics for non-classical aileron buzz analysis. In *International Forum on Aeroelasticity and Structural Dynamics*. Bristol, UK.

[7] Muffo, D., Quaranta, G., Guardone, A., et al. (2007). Interface velocity consistency in time-accurate flow simulations on dynamic meshes. Tech. rep., Politecnico di Milano.

[8] Romanelli, G., Serioli, E., and Mantegazza, P. (2010). A 'free' approach to computational aeroelasticity. In *48th AIAA Aerospace Sciences Meeting*.

[9] Howlett, J. T. (1992). Calculations of unsteady transonic flows with mild separation by viscous-inviscid interaction. Tech. rep., NASA Langley Research Center, Hampton, Virginia.

[10] Fusi, F., Romanelli, G., Guardone, A., et al. (2012). Assessment of geometry reconstruction techniques for the simulation of non-classical aileron buzz. ASME International Mechanical Engineering Congress and Exposition, Houston, Texas.

[11] Gelb, A. and Velde, W. E. V. (1968). *Multiple-Input Describing Functions and Nonlinear System Design*. McGraw-Hill Book Company.

[12] Manetti, M., Quaranta, G., and Mantegazza, P. (2009). Numerical evaluation of limit cycles of aeroelastic system. *Journal of Aircraft*, 46(5).

COPYRIGHT STATEMENT